SciMedCentral

Annals of Clinical Pathology

Research Article

KIAA1549-BRAF Fusion-independent *RSK1* over Expression in Pilocytic Astrocytoma

Aušrinė Areškevičiūtė[1], Cathrine Sandager Budtz[2], Karsten Nysom[2], Morten Grauslund[1] and Helle Broholm[1]*

[1]*Department of Pathology, Laboratory for Molecular Pathology, Copenhagen University Hospital, Denmark*

[2]*Department of Pediatrics and Adolescent Medicine, Section of Pediatric Hematology and Oncology, The Juliane Marie Centre, Denmark*

***Corresponding author**

Helle Broholm, Department of Pathology, Consultant Neuropathologist, Copenhagen University Hospital, 5443, The Center of Diagnostic Investigation, Rigshospitalet, Blegdamsvej 9, Copenhagen 2100, Denmark; Tel: 45 -35456336; Fax: 45-35455431; Email: helle.broholm@regionh.dk

Submitted: 31 December 2015

Accepted: 14 February 2016

Published: 16 February 2016

ISSN: 2373-9282

Keywords

- RSK expression
- KIAA1459
- BRAF fusion gene
- pilocytic astrocytoma
- MAP kinases

Abstract

BRAF is the most frequently altered gene in pediatric low grade glioma (pLGG), primarily in the most common pLGG – the pilocytic astrocytoma (PA) harboring a tandem duplication on chromosome 7q34 which results in the *KIAA1549 – BRAF* fusion gene. The rates of *BRAF* fusion are depending on tumor location in the CNS and the prognostic effects of this fusion are variable. *BRAF* fusion proteins result in aberrant activation of the MAP-Kinase (MAPK) pathway, downstream of which the p90 Ribosomal S6 kinase (RSK) is located, known to be important for regulation of gene expression and protein synthesis. However, *RSK* genes activity, and their relation to the major molecular event in PA pathogenesis – the *KIAA1549-BRAF* genes fusion has never been investigated. Fifty patients with a total number of 73 tumor samples were included in the study: 52 formalin-fixed paraffin-embedded (FFPE) and 21 corresponding fresh frozen (FF) tumor samples of various pLGG and high-grade glioma (HGG). q-PCR and RT-PCR were performed in order to quantify *RSK* expression and the presence of *BRAF* fusion gene, respectively. PCR products were subjected to gel electrophoresis and Sanger sequencing. Immunohistochemistry and Western Blotting were performed for RSK proteins investigation. Interestingly, *RSK1* expression was 3.485 times increased in PAs compared to normal tissue. The change in *RSK1* expression had no correlation with the status of *KIAA1549-BRAF* fusion presence.

ABBREVIATIONS

PA: Pilocytic Astrocytoma; **MAPK:** Mitogen Activated Protein Kinase; **RSK:** Ribosomal S6 protein Kinase; **BRAF:** B-Raf proto oncogene, serine/threonine kinase; **LGG:** Low-Grade Glioma

INTRODUCTION

Pilocytic astrocytoma (PA) is the most common pediatric low-grade glioma (pLGG), constituting 23% of all central nervous system (CNS) tumors in children [1]. According to World Health Organization (WHO) classification, PA is a grade I tumor [2]. It has no gender preponderance and mainly occurs in children from 5 to 19 years old with a peak incidence in the 5 to 9 years old range [3]. Even though PA is a well- circumscribed tumor, with a 10-year survival of 96% after tumor resection, recurrence occurs in 19% of cases, often when the tumor is not completely rejected [4]. Pontine and optic pathway's PAs are the most complicated and difficult to reset, thus children may experience significant morbidity due to tumor's location and/or the side effects of adjuvant therapies. PA is morphological a heterogeneous tumor with the classical histological features being elongated bipolar tumor cells, Rosenthal fibers, and eosinophilic granular bodies (Figure 1) [5]. However, the diagnosis can be challenging when necrosis and vascular proliferation is present, which do not always imply an unfavorable prognosis [6,7].

The MAPK pathway is composed of the Ras/Raf/MEK/ERK kinases. It is critical for normal development and is deregulated in a multitude of cancers and neurodegenerative diseases e.g. Alzheimer's and Parkinson's disease [8]. The *BRAF* gene is one of the genes most frequently affected by cancerous mutations, and the most common mutation is the BRAF V600E substitution in the tyrosine kinase domain of the protein [9]. In up to 80% of PAs tandem duplication of chromosome 7q34 occurs, resulting in the formation of a fusion gene between the kinase domain of *BRAF* and *KIAA1549* (*KIAA1549-BRAF* fusion gene), leading

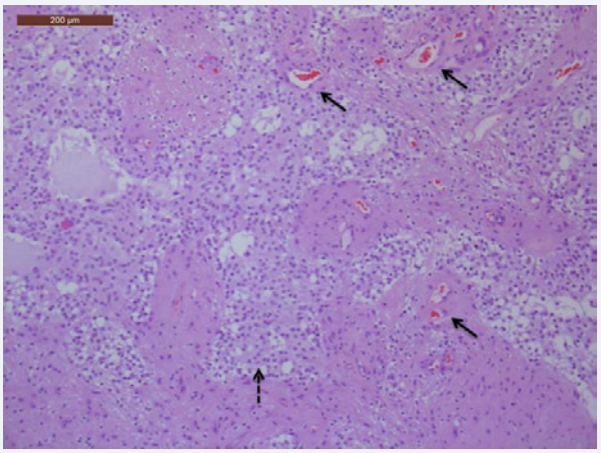

Figure 1 Pilocytic astrocytoma - biphasic tumor tissue with uniform tumor cells with clear cytoplasm (dotted arrow) and hyperplastic vessels (black arrow) - H&E staining (x200).

to constitutively active MAPK pathway [10,11]. There are different fusion variants, which are distinguished according to the fusion sites. The most common *KIAA1549-BRAF* fusions in PA are between the *KIAA1549* exon 16 and *BRAF* exon 9 (16-9) in up to 77% of PAs, *KIAA1549* exon 15 and *BRAF* exon 9 (15-9) - 28%, and *KIAA1549* exon 16 and *BRAF* exon 11 (16-11) - 5%. [7,12]. However, as growing evidence suggest, MAPK pathway is aberrantly activated in all PA regardless of 7q34 duplication and a number of less frequent somatic mutations in BRAF, KRAS, NF1, FGFR1 as well as other BRAF or NTRK2 fusions [13,14]. This indicates that several different genes could be involved in the MAPK pathway´s proteins production, and that they may influence PA pathogenesis.

The 90 kDa ribosomal S6 protein kinases (RSKs), are a family of Ser/Thr kinases that are activated by the MAPK pathway (Figure 2) [15]. The RSK kinase family consists of four isoforms (RSK1-4) which are highly homologous with up to 90% amino acid identity among the protein sequences [16]. RSK family members phosphorylate many substrates that are in charge of cell growth, proliferation, cell cycle progression, and motility [17]. RSKs are recognized as influential proteins in various cancers and neurodegenerative diseases, e.g. mutations in *RSK2*, which lead to aberrant protein activity, are associated with Coffin-Lowry syndrome, an X-linked disorder with severe psychomotor retardation [18]. However, little is known about RSK function, cellular distribution and role in human brain tumors [19].

The best characterized RSK isoforms in other diseases - *RSK1* and *RSK2* - are of special interest, and to our knowledge, their activity in PA has not been studied before. Therefore, we hypothesized that *RSK* genes expression would be abnormal and that RSK proteins, which are BRAF downstream effectors, would be aberrantly regulated in PA.

MATERIALS AND METHODS

Material

All patients included in this study were diagnosed and treated at Rigshospitalet, Copenhagen University Hospital. The material includes 73 tumor samples from 50 patients (24 males) with a median age of 10years (range 0 to 17). Fifty-two formalin-fixed paraffin-embedded (FFPE) and 21 corresponding fresh frozen (FF) tumor samples of various pLGG and HGG were collected from the archives of the Department of Neuropathology, Rigshospitalet, Denmark (Table 1). Of the 21 FF samples, 16 were pilocytic astrocytomas, 7 males and 9 females, with age median of 10 years at diagnosis. As *KIAA1549-BRAF* 15-9 fusion is associated with tumor location [20], the distribution of the 16 PAs is listed in (Table 2). The tumors were located in fossa posterior – (9 PA), pontine (3PA), supratentorial above 3rd ventricle (1PA), basal ganglia (1PA), in the medulla oblongata (1PA) and in infra- and supratentorial region (1PA) (Table 2). All tissue samples were collected from patients in accordance with the Declaration of Helsinki and with approval by the Medical Ethics Committees of the Capital Region, Denmark (approval no. H-3-2013-195). All tumors were classified according to the 2007 WHO classification [2].

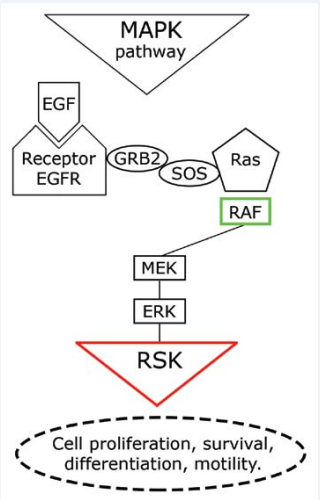

Figure 2 Schematic MAPK pathway - RSK place in the MAPK pathway and its function in the cell.

Table 1: The number of FF and FFPE samples in the study.

FF		
Diagnose	**WHO grade**	**Samples**
Pilocytic astrocytoma	I	16
Ependymoma	II	2
Oligodendroglioma	II	1
Diffuse astrocytoma	II	2
FFPE		
Pilocytic astrocytoma	I	27
Ependymoma	II	4
Oligodendroglioma	II	4
Diffuse astrocytoma	II	3
Anaplastic ependymoma	III	3
Ana plastic oligodendroglioma	III	1
Glioblastoma	IV	10

Abbreviations: FF: Fresh Frozen; **FFPE:** Formalin-Fixed and Paraffin Embedded; **WHO:** World Health Organization

Table 2: PA patient's gender, age, tumor location, *KIAA1549-BRAF* gene fusion site - if any, and *RSKs* expression presented as the number of cycles required for the fluorescent signal to cross the threshold.

	Gender	Age	PA location	*KIAA1549-BRAF* fusion site	*RSK1* Ct (n=2)	*RSK2* Ct (n=2)
1.	M	8	Supra-cellular above 3rd ventricle	16-11	32.36	31.74
2.	F	13	Pontine	16-11	31.53	27.67
3.	F	10	Fossa posterior	16-9/15-9	33.43	34.54
4.	F	14	Fossa posterior	negative	30.79	30.44
5.	F	4	Right basal ganglia	unknown	31.22	30.32
6.	M	8	Fossa posterior	unknown	31.05	28.98
7.	F	16	Fossa posterior	negative	29.38	28.18
8.	F	9	Fossa posterior	15-9	33.36	31.95
9.	F	17	Fossa posterior	16-9	30.05	30.45
10.	F	1	Medulla oblongata	16-11	30.75	30.41
11.	M	10	Fossa posterior	16-11	29.55	28.95
12.	M	9	Fossa posterior	unknown	29.14	28.83
13.	M	14	Pontine	16-9	31.73	32.05
14.	M	7	Pontine	16-11/16-9	27.09*	26.41*
15.	M	13	Infra- and supratentorial	16-9	29.74	28.28
16.	F	12	Fossa posterior	16-9	28.67	28.75

Abbreviations: M: Male; **F**: Female; **Ct:** Cycle threshold; **n=2:** average of two q-PCR runs data; ***n=1**: one q-PCR run data.

METHODS

Polymerase chain reaction (PCR)

For *RSK1* and *RSK2* expression, RNA was purified from approximately 30 mg of all FF tissues by the use of the All Prep DNA/RNA/Protein Mini Kit (Cat.No.80004 Qiagen, Hilden, Germany) according to manufacturer's recommendations. RNA was also isolated from FFPE tissues (RNeasy FFPE Kit (Cat. No.73504 Qiagen, Hilden, Germany), however, the quality of this RNA was not good enough for further molecular investigation. FF brain tissues from epileptic surgery operations with no histopathological changes were obtained from 7 patients and used as normal controls. By quantitative real-time PCR (q-PCR) the expression of *RSK1*, *RSK2* and the housekeeping gene *GAPDH* was evaluated. RNA from the 21 FF tumors was converted to cDNA by using the SABiosciences® RT^2 First Strand Kit (Cat. No.330401, Qiagen) and Quantitect® First Strand Kit, Reverse Transcription Kit (Cat.No.205311, Qiagen). RNA and cDNA concentrations were measured by using NanoDrop 2000 spectrophotometer (Thermo Science). TaqMan® Universal Master Mix II with UNG (Part.No.4440038) and Gene expression assays (Hs01546665_m1 RPS6KA1, Hs00177936_m1 RPS6KA3, and Hs02758991_g1 GAPDH, LifeTechnologies) were used for cDNA amplification. The volume for each amplification reaction was totally 20 µL, which consisted of 10 µL of TaqMan® Universal Master Mix II, with UNG; 1 µL of TaqMan® Gene Expression Assay, 4 µL of cDNA template and 5µL of RNase-free water. Three assays were performed at least 3 times for each sample. q-PCR was performed using a Rotor-Gene Q (Qiagen) real-time PCR instrument. Samples were first incubated at 50°C for 2 min, then at 95°C for 10 min, followed by 40 cycles of 95°C for 15 s and 60°C for 1 min. Fluorescence was recorded and cycles to thresholds (Ct) were calculated using Rotor-Gene Q Series Software version 2.1.0. (Qiagen). The REST-384-beta software (Pfaffl and Horgan, 2006) was used to calculate the relative expression ratio of a target gene versus reference gene - GAPDH [21]. The calculation is based on ΔΔ Ct method, where the target genes amplification efficiency was 1.7 per one PCR cycle as reported by Rotor-Gene Comparative Quantification software after PCR performance. Agarose gel electrophoresis with q-PCR products was performed to validate RNA presence and its amplification (Figure 3).

To study whether *RSK* expression in PA was influenced by the presence of *KIAA1549-BRAF* fusion, RT-PCR was performed with 15/16 FF PA samples. cDNA was synthesized using the Affinity Script QPCR Synthesis Kit (Cat.No.600559) from Agilent Technologies and the Bio-Rad S1000TH Thermal Cycler machine. Forward and reverse primers' sequences, as well as the protocol for *KIAA1549-BRAF* fusion detection described by Jones and Hasselblatt (Table 3) were used with minor adjustments in the number of PCR cycles (increased to 45) and temperature (decreased in 2°C in step 3) [7,22]. As a positive control 215 base pairs fragment of the endogenous *BRAF* was used. FF tissue from breast, brain, colon, lymph node and thyroid were used for reduction of the background noise and as a negative control for *KIAA1549-BRAF* detection. PCR products were subjected to Qiaxcell's Gel Electrophoresis to detect fusions by measuring band sizes of the amplified fragments. In concordance, Sanger sequencing was performed on 8 PCR product samples, from 2 of each: positive endogenous controls, positive 16-9, 15-9 and 16-11 fusions. The sequencing indicated the presence of the expected *BRAF* alleles, and thereby validated the respective fragment sizes as *BRAF* fusions.

Immunohistochemistry(IHC)

In order to identify the presence and location of the RSK proteins within the tumor tissue, immunohistochemistry

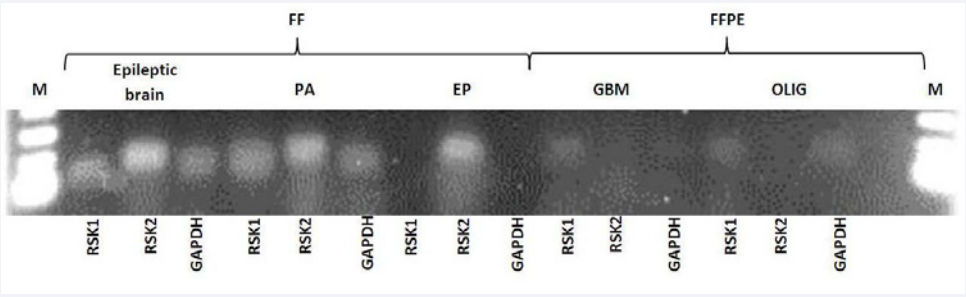

Figure 3 Agarose gel electrophoresis with q-PCR amplification products of RSK1, RSK2 and GAPDH primers from FF (left) and FFPE (right) tissues: epileptic brain (control); PA: Pilocytic Astrocytoma; EP: Ependymoma; GBM: Glioblastoma; OLIG: Oligodendroglioma; M: Marker.

Table 3: *KIAA1549* and *BRAF* fusion genes primer sequences.

Primer name	RT-PCR
BRAF_9_F	5′-AAACAGCACCCCTTCCCAGG-3′
BRAF_11_F	5′-CGGAAACACCAGGTCAACGG-3′
KIAA1549_16_R	5′-CTCCATCACCACGAAATCCTTG-3′
KIAA1549_15_R	5′-GTTCCAAATGATCCAGATCCAATTC-3′
Positive control	
BRAF	5′-TTGTGACTTTTGTCGAAAGCTGC-3′
KIAA1549	5′-AAGGGGATGATCCAGATGTTAGG- 3′

Abbreviations: Primers nucleotide sequences of the 3 most common *KIAA1549-BRAF* fusion exon sites, and the positive control – endogenous *BRAF*.

was performed on 4 µm sections on all 52 FFPE tumors. After deparaffinization in xylene, the sections were hydrated in 100, 90, 70% ethanol and pretreated with Tris buffer pH 8.5 for antigen retrieval. The primary and secondary antibody combinations used were Anti-RSK1 p90 rabit-monoclonal antibody ([E4]ab32114, Lot: GR41669-7) (1:25 dilution) and Anti-Rsk2/ MAPKAP Kinase 1b rabit-monoclonal antibody ([Y83]ab32133, Lot: GR20999-5) (1:50 dilution) (both from Abcam) and Optiview (Roche). DAB (3,3'-Diaminobenzidine, Roche) was applied for visualization. All reactions were run on a Benchmark IHC staining module (Ventana Medical System, Tuscon, AZ, USA) and were evaluated by a senior neuropathologist (HB).

Western Blot (WB)

WB was performed with the same RSK antibodies that were used for IHC, in order to validate their specificity. FF tissues from epileptic brain (E), normal colon tissue (C), glioblastoma (GMB), and colon cancer (CC), were placed in Eppendorf tubes with extraction buffer and homogenized manually. Epileptic brain tissue was expected to contain smaller amount of RSK proteins compared to colon cancer tissue. The weight of the tissue and volume of extraction buffer were equalized to 1:1. Protein concentration was measured by using the Qubit® Protein Assay Kit (cat#Q33211, LifeTechnologies) on a Qubit® 2.0 Fluorometer (LifeTechnologies) according to the manufacturer's manuals. Samples, which protein concentration was >26 µg/µL, were diluted in the extraction buffer to 1:5, 1:10 and 1:100. Before loading samples into the gel, they were mixed with sample loading buffer and sample reducing agent, and heated at 99°C for 10 min. SeeBlue visual marker and MagicMark XP marker (Invitrogen) were used as a standard protein ladder. Gel electrophoresis was run for 1.5 h at 100 V. Proteins from the gel were transferred to nitrocellulose membrane in Transfer buffer at 30 V for 1.5 h. Final blots were immunoblotted with the Anti-RSK1 p90 (1:700 and 1:1000 dilution) and Anti-Rsk2/ MAPKAP Kinase 1b (1:1500 dilution) primary antibodies (Abcam). Stabilized Goat Anti-Rabbit antibody (HRP) (1:50 dilution) was used as secondary antibody (Pierce®). Pierce® ECL Western Blotting Substrate (1:1 dilution) was used to enhance chemiluminescence of the secondary antibody. Proteins were detected with Versa Doc imaging system using Quantity One software (Bio-Rad).

Statistics

The REST-384-beta software (Pfaffl and Horgan, 2006) was used for calculation of RSK relative expression ratio significance (p value). *RSK* expression changes in relation to *KIAA1459-BRAF* positive, negative, unknown status was evaluated with the analysis of variance (ANOVA) using SAS statistical software version 9.1 (SAS Institute, Cary, NC)).

RESULTS AND DISCUSSION

Results

RSK1 and RSK2 expression: *RSK1* measured by q-PCR was significantly over expressed by the factor 3.485 (SE±1.68) in all 16 PA tumors compared to 7 controls (p=0.001). *RSK2* also tended to be over expressed, but the difference, compared to control group, was not significant (Figure 4).

The other 5 FF gliomas, which were tested for *RSKs* expression, were 2 diffuse astrocytomas, 2 ependymomas, and 1 oligodendroglioma – all WHO grade II. No significant difference in *RSKs* expression in diffuse astrocytoma and ependymoma samples compared to control group was found, however *RSK1* and *RSK2* tended to be over expressed in diffuse astrocytomas, and under expressed in the ependymoma. One oligodendroglioma

showed significant 2.8 fold *RSK1* over expression compared to control group (p=0.011) (data not shown).

***KIAA1549-BRAF* fusion & RSK expression:** Fifteen FF PAs were tested for *KIAA1549-BRAF* gene fusions, of which 11were *KIAA1549-BRAF* fusion positive, 2 negative, and 3 unknown (including 1 PA that was not tested for the fusion) (Table 2). ANOVA was performed to evaluate if *RSK1* and *RSK2* gene expression in 15 PAs differ significantly depending on whether *KIAA1549-BRAF* gene fusion is positive, negative or unknown. The p values for *RSK1* (p=0.77) and *RSK2* (p=0.87) indicated that level of *RSK* expression does not vary according to *KIAA1549-BRAF* gene fusion positive, negative and unknown groups (Figure 5).

RSK proteins in pilocytic astrocytoma: Despite great optimization effort and specific IHC staining in normal colon tissue, used as control for RSK1 antibody, and lymph node for RSK2 antibody, it was impossible to prevent background staining in tissues from CNS: neither in controls (glioblastoma), nor the tumors tested, especially regarding the RSK1 staining. In all sections a granular RSK1 staining was found clearly in the cytoplasm of endothelial cells and RSK2 staining in the cytoplasm of microglia and macrophages, both perivascular and more diffusely distributed. Because of background staining with the RSK1 antibody, and a more often negative staining with the RSK2 antibody (Figure 6) the results were difficult to judge as reliable and therefore not further explored. In accordance with the IHC observation, WB resulted in multiple binding of different size proteins for RSK1 (1:700 and 1:1000 dilution) and RSK2 (1:1500 dilution) antibodies (Abcam) (strongest to 55 kDa) in positive control tissues as well as LGG (Figure 7). However, both RSK1 and RSK2 proteins naturally are of 84 kDa size.

Discussion

The data presented in this study demonstrate that in all investigated PAs (16), *RSK1* expression is found significantly increased (3.485 times) compared to control. The data also suggest that *RSK1* might be regulated in a *KIAA1549-BRAF*-fusion-independent manner, because no correlation between fusion status and *RSK* expression was found, even though *BRAF* fusion genes are recognized as the key oncogenic mechanism. Nevertheless, it is known that MAPK pathway is also constantly active in PAs that have no BRAF, KRAS, NF1, FGFR1 or NTRK2 fusions and/or mutations. Therefore, we propose that *RSK1* over expression in PA might be triggered by other factors than

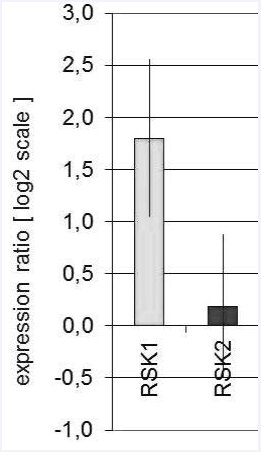

Figure 4 Relative *RSK1* and *RSK2* expression ratio plot [mean ± S.E.], PAs compared to control group, log2 scale..

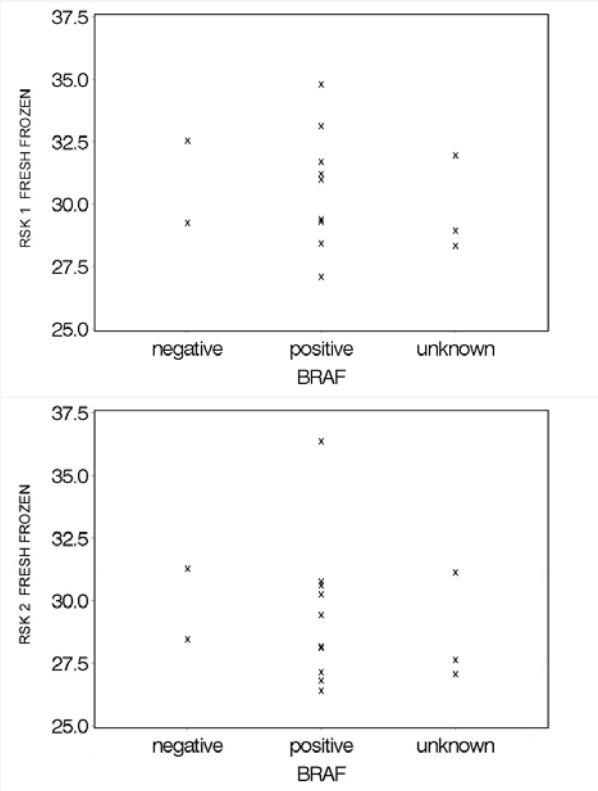

Figure 5 *RSK1* and *RSK2* expression variation in *KIAA1549-BRAF* gene fusion negative, positive and unknown groups.

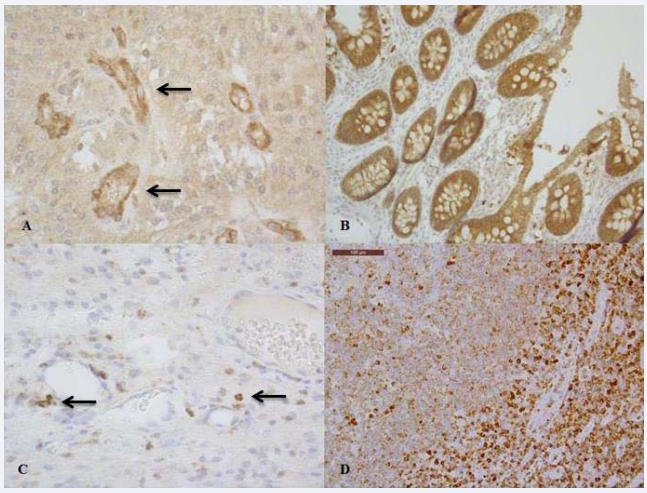

Figure 6 (A) - Background staining, but clearly visible RSK1 antibody positive endothelial cells around the vessels in PA (arrows) (x400); (B) - RSK1 antibody validation on colon tissue (x200); (C) - RSK2 positive microglial cells and macrophages in PA (arrows) (x400); (D) - RSK2 antibody validation on lymphnode tissue (x100).

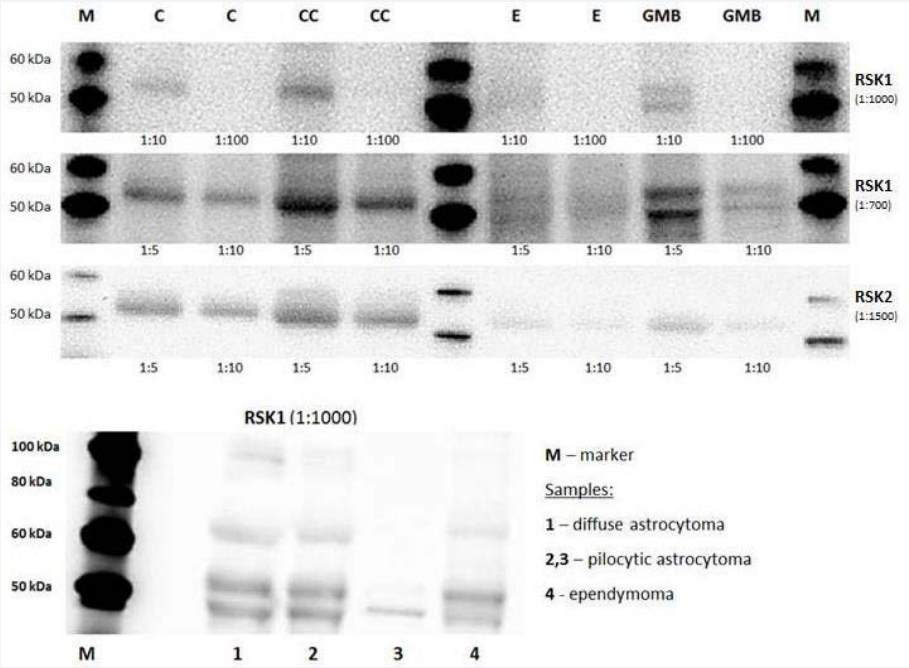

Figure 7 RSK1 and RSK2 antibody optimization for Western Blot analysis. Positive control specimens: **C:** colon; **CC:** Colon Cancer; **E:** Epileptic brain tissue without pathological changes; **GBM:** Glioblastoma. Pathological specimens: 1 – diffuse astrocytoma, 2, 3 – pilocytic astrocytoma, 4 – ependymoma. M – Marker.

BRAF fusion gene induced constitutive MAPK pathway activation. However, which other genes, proteins and their overlapping pathways cause *RSK1* over expression remains to be elucidated.

Not much is known about *RSK* expression in human CNS tumors, but similar observation regarding to *RSK* independent activity was made by Clark et al., who provide evidence of MAPK-independent *RSK* activity in prostate cancer. They demonstrates that *RSK2* activity in response to epithelial growth factor (EGF) is 35-fold greater in PC-3 than LNCaP cells, even though active MAPK and 3-Phosphoinositide-dependent protein kinase-1 (PDK1) levels are lower in PC-3 cells, meaning that increased *RSK* levels are not a reflection of major regulatory inputs such as MAPK and PDK1 [23].

Extracellular-signal regulated kinases of the MAPK pathway, such as Ras, Raf1, MEK and ERK, are being intensively investigated as growing evidence indicate their over expression and activation being an important part of human colorectal and prostate cancer pathogenesis, progression, and oncogenic behavior [23-25]. Regarding PA, the identification of novel *BRAF* fusion partners, such as *FAM131B* and *SRGAP3*, has provided evidence of RAF kinase fusion genes playing a key role in the constitutive activation of the MAPK pathway's [26].

To understand the MAPK-RSK signal-transduction pathways, most of the studies are conducted in melanoma, pancreatic, breast, prostate and small cell lung cancer lines, confirming that the abnormal *RSK1* and *RSK2* expression is crucial for tumor cells proliferation and invasion [27-29]. Expression of other *RSK* family members is found to be aberrant and significant for tumor development and/or suppression as well: *RSK3* is reduced or absent in ovarian cancer cell lines, and *RSK4* is over expressed in the human breast cancer cell line MDA-MB-231 [29]. Meanwhile the biological implication of *RSK* over expression in CNS tumors remains to be clarified, especially when specific inhibitors of RSK (SLO101, BI-D1870) have been identified and new ones are under development (bis-phenol pyrazole, LJI308) [30- 33]. In 2013 a research group in Canada (Pambid et al.) identified RSK as a crucial target for pediatric Sonic Hedgehog medulloblastoma (SHH MB), as they found MB cell lines (Daoy, ONS76, UW228, UW426) being resistant to SHH pathways' smoothened (SMO) inhibitors. RSK inhibition with BI-D1870 resulted in prevention of Daoy colony formation by ~100%. They also found that *RSK2-4* are correlated with SHH genes, and were consistently expressed higher in MB patients compared to normal cerebellum [34]. However, this was not the case for *RSK1*, which might be rather associated with LGG as our study suggests.

CONCLUSION

The finding of increased *RSK1* expression in PA is promising and opens door for further investigations of genetic and epigenetic factors considering *KIAA1549-BRAF*-independent *RSK1* upstream components, causing its increased expression without changing its genetic code. The molecular genetic changes in pediatric CNS tumors differ from that in adults, so *RSK* expression should be investigated in a large cohort of gliomas of different grades and in different age group for better understanding of the MAPK-RSK pathway, its function in tumorigenesis and novel targets for biomarker and treatment options. A range of promising RSK inhibitors, such as luteolin, dibenzyl trisulfide (DTS), small molecule inhibitor SLO101 and BI-D1870 in combination with other cancer agents are adapted and applied for different types of cancer treatment and opens the possibility for PA personalized therapy in the future [35,36].

ACKNOWLEDGEMENTS

We thank Søren Skov, Lars Peter Sørensen, Henrik Dyrbye, Elena Projva, and Jan Lauritzen for guidance and technical support.

REFERENCES

1. Laviv Y, Toledano H, Michowiz S, Dratviman-Storobinsky O, Turm Y, Fichman-Horn S, et al. BRAF, GNAQ, and GNA11 mutations and copy number in pediatric low-grade glioma. FEBS Open Bio. 2012; 2: 129-134.
2. Louis DN, Ohgaki H, Wiestler OD, Cavenee WK, Burger PC, Jouvet A, et al. The 2007 WHO classification of tumours of the central nervous system. Acta Neuropathol. 2007; 114: 97-109.
3. Sievert AJ, Fisher MJ. Pediatric low-grade gliomas. J Child Neurol. 2009; 24: 1397-1408.
4. Dirven CM, Mooij JJ, Molenaar WM. Cerebellar pilocytic astrocytoma: a treatment protocol based upon analysis of 73 cases and a review of the literature. Childs Nerv Syst. 1997; 13: 17-23.
5. Jones DT, Kocialkowski S, Liu L, Pearson DM, Ichimura K, Collins VP. Oncogenic RAF1 rearrangement and a novel BRAF mutation as alternatives to KIAA1549: BRAF fusion in activating the MAPK pathway in pilocytic astrocytoma. Oncogene. 2009; 28: 2119-2123.
6. Sadighi Z, Slopis J. Pilocytic astrocytoma: a disease with evolving molecular heterogeneity. J Child Neurol. 2013; 28: 625-632.
7. Jones DT, Kocialkowski S, Liu L, Pearson DM, Bäcklund LM, Ichimura K, et al. Tandem duplication producing a novel oncogenic BRAF fusion gene defines the majority of pilocytic astrocytomas. Cancer Res. 2008; 68: 8673-8677.
8. Kim EK, Choi EJ. Pathological roles of MAPK signaling pathways in human diseases. Biochim Biophys Acta. 2010; 1802: 396-405.
9. Dhillon AS, Hagan S, Rath O, Kolch W. MAP kinase signalling pathways in cancer. Oncogene. 2007; 26: 3279-3290.
10. Pfister S, Janzarik WG, Remke M, Ernst A, Werft W, Becker N, et al. BRAF gene duplication constitutes a mechanism of MAPK pathway activation in low-grade astrocytomas. J Clin Invest. 2008; 118: 1739-1749.
11. Becker AP, Scapulatempo-Neto C, Carloni AC, Paulino A, Sheren J, Aisner DL, et al. KIAA1549: BRAF Gene Fusion and FGFR1 Hotspot Mutations Are Prognostic Factors in Pilocytic Astrocytomas. J Neuropathol Exp Neurol. 2015; 74: 743-754.
12. Marko NF, Weil RJ. The molecular biology of WHO grade I astrocytomas. Neuro Oncol. 2012; 14: 1424-1431.
13. Jacob K, Albrecht S, Sollier C, Faury D, Sader E, Montpetit A, et al. Duplication of 7q34 is specific to juvenile pilocytic astrocytomas and a hallmark of cerebellar and optic pathway tumours. Br J Cancer. 2009; 101: 722-733.
14. Jones DT, Hutter B, Jäger N, Korshunov A, Kool M, Warnatz HJ, et al. Recurrent somatic alterations of FGFR1 and NTRK2 in pilocytic astrocytoma. Nat Genet. 2013; 45: 927-932.
15. Romeo Y, Zhang X, Roux PP. Regulation and function of the RSK family of protein kinases. Biochem J. 2012; 441: 553-569.
16. Lara R, Seckl MJ, Pardo OE. The p90 RSK family members: common functions and isoform specificity. Cancer Res. 2013; 73: 5301-5308.
17. Aronchik I, Appleton BA, Basham SE, Crawford K, Del Rosario M, Doyle LV, et al. Novel potent and selective inhibitors of p90 ribosomal S6 kinase reveal the heterogeneity of RSK function in MAPK-driven cancers. Mol Cancer Res. 2014; 12: 803-812.
18. Jacquot S, Zeniou M, Touraine R, and Hanauer A. X-linked Coffin-Lowry syndrome (CLS, MIM 303600, RPS6KA3 gene, protein product known under various names: pp90rsk2, RSK2, ISPK, MAPKAP1). Eur J Hum Genet. 2002; 10: 2-5.
19. Broholm H, Gammeltoft S. In Situ Reverse Transcription PCR for Detection of mRNA in the CNS. Cellular and Molecular Methods in Neuroscience Research. 2002; 9: 145-159.
20. Faulkner C, Ellis HP, Shaw A, Penman C, Palmer A, Wragg C, et al. BRAF Fusion Analysis in Pilocytic Astrocytomas: KIAA1549-BRAF 15-9 Fusions Are More Frequent in the Midline Than Within the Cerebellum. J Neuropathol Exp Neurol. 2015; 74: 867-872.
21. Pfaffl MW, Horgan GW, Dempfle L. Relative expression software tool (REST) for group-wise comparison and statistical analysis of relative expression results in real-time PCR. Nucleic Acids Res. 2002; 30: 36.
22. Hasselblatt M, Riesmeier B, Lechtape B, Brentrup A, Stummer W, Albert FK, et al. BRAF-KIAA1549 fusion transcripts are less frequent in pilocytic astrocytomas diagnosed in adults.Neuropathol Appl Neurobiol. 2011; 37: 803-806.
23. Clark DE, Errington TM, Smith JA, Frierson HF, Weber MJ, Lannigan DA. The serine/threonine protein kinase, p90 ribosomal S6 kinase, is an important regulator of prostate cancer cell proliferation.Cancer Res. 2005; 65: 3108-3116.
24. Lemieux E, Cagnol S, Beaudry K, Carrier J, Rivard N. Oncogenic KRAS signalling promotes the Wnt/Î²-catenin pathway through LRP6 in colorectal cancer. Oncogene. 2015; 34: 4914-4927.
25. Fang JY, Richardson BC. The MAPK signalling pathways and colorectal cancer. Lancet Oncol. 2005; 6: 322-327.
26. Cin H, Meyer C, Herr R, Janzarik WG, Lambert S, Jones DTW, et al. Oncogenic FAM131B–BRAF fusion resulting from 7q34 deletion comprises an alternative mechanism of MAPK pathway activation in pilocytic astrocytoma. Acta Neuropathol.2011; 121: 763-774.
27. Lommel MJ, Trairatphisan P, Gäbler K, Laurini C, Muller A, Kaoma T, et al. L-plastin Ser5 phosphorylation in breast cancer cells and in vitro is mediated by RSK downstream of the ERK/MAPK pathway. FASEB J. 2015.
28. Eisinger-Mathason TS, Andrade J, Lannigan DA. RSK in tumorigenesis: connections to steroid signaling. Steroids. 2010; 75: 191-202.
29. Eisinger-Mathason TS, Andrade J, Groehler AL, Clark DE, Muratore-Schroeder TL, Pasic L, et al. Codependent functions of RSK2 and the apoptosis-promoting factor TIA-1 in stress granule assembly and cell survival. Mol Cell. 2008; 31: 722-736.
30. Shiota M, Yokomizo A, Takeuchi A, Itsumi M, Imada K, Kashiwagi E, et al. Inhibition of RSK/YB-1 signaling enhances the anti-cancer effect of enzalutamide in prostate cancer. Prostate. 2014; 74: 959-969.
31. Chiu CF, Bai LY, Kapuriya N, Peng SY, Wu CY, Sargeant AM, et al. Antitumor effects of BI-D1870 on human oral squamous cell carcinoma. Cancer Chemother Pharmacol. 2014; 73: 237-247.
32. Jain R, Mathur M, Lan J, Costales A, Atallah G, Ramurthy S, et al. Discovery of Potent and Selective RSK Inhibitors as Biological Probes. J Med Chem. 2015; 58: 6766-6783.
33. Davies AH, Reipas K, Hu K, Berns R, Firmino N, Stratford AL, et al. Inhibition of RSK with the novel small-molecule inhibitor LJI308 overcomes chemo resistance by eliminating cancer stem cells. Oncotarget. 2015; 6: 20570-20577.
34. Pambid MR, Berns R, Adomat HH, Hu K, Triscott J, Maurer N, et al. Overcoming Resistance to Sonic Hedgehog Inhibition by Targeting p90 Ribosomal S6 kinase in Pediatric Medulloblastoma. Pediatr Blood Cancer. 2014; 61: 107-115.

35. Reipas KM, Law JH, Couto N, Islam S, Li Y, Li H, et al. Luteolin is a novel p90 ribosomal S6 kinase (RSK) inhibitor that suppresses Notch4 signaling by blocking the activation of Y-box binding protein-1 (YB-1). Oncotarget. 2013; 4: 329-345.

36. Lowe HI, Facey CO, Toyang NJ, Bryant JL. Specific RSK kinase inhibition by dibenzyl trisulfide and implication for therapeutic treatment of cancer. Anticancer Res. 2014; 34: 1637-1641.

Cite this article

Areškevičiūtė A, Budtz CS, Nysom K, Grauslund M, Broholm H (2016) KIAA1549-BRAF Fusion-independent RSK1 over Expression in Pilocytic Astrocytoma. Ann Clin Pathol 4(2): 1064.